# Cu(II) Ion Adsorption Using Activated Carbon Prepared from Pithecellobium Jiringa (*Jengkol*) Shells with Ultrasonic Assistance: Isotherm, Kinetic and Thermodynamic Studies

**Abrar Muslim[1,*], Ellysa[2] & Syahiddin Dahlan Said[1]**

[1]Process Technology Laboratory, Department of Chemical Engineering, Syiah Kuala University, No.7 Jalan Tgk. Syech Abdul Rauf, Darussalam, Banda Aceh, Indonesia
[2]Baristand Industri Banda Aceh, Ministry of Industry of Indonesia, Jalan Cut Nyak Dhien No. 377, Lamteumen Timur Banda Aceh, Indonesia
*E-mail: abrar.muslim@che.unsyiah.ac.id

**Abstract.** Adsorption of Cu(II) ions from aqueous solution onto activated carbon (AC) prepared from Pithecellobium jiringa shell (PJS) waste was investigated by conducting batch mode adsorption experiments. The activation with ultrasound assistance removed almost all functional groups in the PJS-AC, while more cavities and pores on the PJS-AC were formed, which was confirmed by FTIR and SEM analyses. The Cu(II) ion adsorption isotherm fitted best to the Freundlich model with average $R^2$ at 0.941. It was also correlated to the Langmuir isotherm with average $R^2$ at 0.889. This indicates that physical sorption took place more than chemical sorption. The maximum Cu(II) ion adsorption capacity onto the PJS-AC for a dose of 1 g was 104.167 mg/g at 30 °C and pH 4.5, where the Langmuir constant was 0.523 L/mg, the Freundlich adsorption intensity was 0.523, and the Freundlich constant was 5.212 L/mg. Cu(II) adsorption followed the pseudo second-order kinetic (PSOKE) model with average $R^2$ at 0.998, maximum adsorption capacity at 96.154 mg/g, PSOKE adsorption rate constant at 0.200 g/mg.min, temperature at 30 °C and pH at 4.5. The changes in enthalpy, entropy, free energy and activation energy were determined, and the results confirmed that Cu(II) adsorption onto the PJS-AC was exothermic chemical adsorption in part. There was a decrease in the degree of freedom and the adsorption was non-spontaneous.

**Keywords:** *activated carbon; isotherm; jengkol (Pithecellobium jiringa); kinetic; thermodynamic; ultrasound.*

## 1 Introduction

Heavy metals can be released into the environment through wastewater of mining operations, petroleum refining, and metallurgical, educational and agricultural industries [1-6]. Among the pollutants, Cu(II) ions are noted as the most toxic to the human body, causing disorders of tissues and organs [7-8].

Received February 26th, 2017, 1st Revision May 8th, 2017, Accepted for publication October 2nd, 2017.
 ISSN: 2337-5779, DOI: 10.5614/j.eng.technol.sci.2017.49.4.4

Cu(II) ions are generally found in the wastewater of chemical industries, mining practice, and electrical industries [9].

Adsorption is a promising process to reduce heavy metal ions from wastewater compared to other processes being applied because the adsorption process is simpler, more economical and more effective [10-12]. Some low-cost adsorbents derived from lignocellulosic materials, such as water melon [13], rice husk [14], Brazil nut shell and tea leaves [15], coffee bean husks [16], areca catechu shell [17], have been applied for the adsorption of Cu(II) ions.

Activated carbon, which has adsorption capacity due to its high porosity and large surface area, can be derived from lignocellulosic materials. It is interesting to note that its global consumption has risen by almost 2 billion tons in 2017 [18]. Activated carbon has been prepared from Cassava peel [19], pecan shell [20], residue of biomass gasification [21], Tunisian date stones [22], hazelnut husks and shell [23-24], corncob [25] and Australian pine cones [26]. Meanwhile, activated carbon prepared from Pithecellobium jiringa shell (PJS-AC) has not yet been investigated for the adsorption of Cu(II) ions.

The Pithecellobium jiringa (*jengkol*) tree is native to primary and secondary forests in Southeast Asian countries including Indonesia (Sumatra, Sulawesi and Kalimantan), Malaysia, Myanmar, Bangladesh and Southern Thailand [27]. PJS waste is an alternative material for preparing activated carbon because the plantation of the *jengkol* tree across Asia, especially in Indonesia, has increased considerably because of the high demand for its seeds for use in foods. *Jengkol* seed production in Indonesia was 62,475, 50,235, 65,830, 62,197 and 61,537 tons in 2009, 2010, 2011, 2012 and 2013, respectively [28]. PJS waste in Indonesia is forecasted to reach 20,000 tons on average every year.

To increase adsorption capacity, several methods of actived-carbon preparation and adsorption conditions have been proposed [29]. Other techniques, such as microwave radiation for chemical activation [30-32] and ultrasound agitation for adsorption, have been investigated. Ultrasound at 20 kHz has been used to restructure active binding sites of sludge to increase Cu(II) adsorption [33]. The waves produced by ultrasound also increase mass transfer in the adsorption process [13,25]. Therefore, it is desirable to apply the ultrasound method in the preparation of PJS-AC.

The research objective of this study was to prepare activated carbon from PJS waste with assistance of ultrasound in the chemical activation. Evaluation of the chemical functional groups and structural characterization of the PJS waste, the PJS carbon and the PJS-AC were performed by Fourier transform infrared spectroscopy (FTIR) and scanning electron microscopy (SEM) analyses. The

effects of contact time, ultrasound assistance, adsorption pH and temperature on the Cu(II) adsorption capacity of the PJS-AC were examined. Isotherm, kinetic and thermodynamic parameters were obtained.

## 2 Experimental Procedure

### 2.1 Preparation of Activated Carbon

PJS waste was collected from Peunayong vegetable market, Banda Aceh, Aceh Province, Indonesia. To prepare the PJS-AC raw material, the same procedure as in the previous study [26] was used. The PJS waste (3 kg) was rinsed using tap water and then dried under the sun for 5 days at an average temperature of 30 °C (± 1 °C) and an average relative humidity of 72% °C (± 5%). Following this it was dried at 120 °C (± 1 °C) for 3 h using an oven drier (NN-ST342M, Memmert, Western Germany). The dried PJS waste was ground to a powder using a dry spice grinder. Pyrolysis of the dried PJS powder was conducted under nitrogen atmosphere at a rate of 5 ml/min in a tube furnace (TF-80/120/160, Human Lab Instrument Co., Korea, 300-1500 °C) with the heating rate at 45 °C/min for 10.5 min. The initial temperature and the final temperature of the system were 28 and 500 °C, respectively. Physical activation was done at 500 °C (± 1 °C) for 0.5 h. The PJS carbon (PJS-C) was then sieved into 60-80 mesh.

Then, 0.05 kg of PJS-C was activated using 500 mL of 0.5 M NaOH (Gatt-Koller, Austria) in a 750-mL beaker glass at a stirring speed of 150 rpm (Compact Magnetic Mini-Stirrer, HI 180-2 F) for 5 h and at 27 °C (± 1 °C). The PJS activated carbon without ultrasonic assistance (PJS-ACWU) was then washed several times using tap water until reaching a neutral pH of 7 (± 0.1), using distilled water at the end. Finally, the PJS-AC was filtered using a vacuum filter and was dried at 110 °C (± 1 °C) for 5 h using the oven drier for removing the excess water. The PJS-ACWU was stored in a sealed bottle for the adsorption experiment. To prepare PJS activated carbon with ultrasonic assistance (PJS-AC), the chemical activation procedure was repeated with the remaining PJS-C (0.05 kg) with ultrasonic assistance at 1 MHz using an ultrasonic probe (13921-05) installed with an Ultrasonic Doppler (13923-99, PHYWE, West Germany).

### 2.2 Preparation of Cu(II) Aqueous Solution

The Cu(II) aqueous solution of 500 mg/L was made by dissolving 4.75 g (±0.01) $CuSO_4.5H_2O$ (99% pure from Aldrich) in 500 mL of distilled water in a 500-mL Erlenmeyer flask. A sample of 2 mL was taken, mixed with 10 mL distilled water and analyzed using an atomic absorption spectrophotometer (AAS) (AA-6300, Shimadzu, Japan) [26]. To determine the real Cu(II)

concentration of the stock solution, the AAS-based Cu(II) concentration was multiplied with a dilution factor of 6. The desired concentration of Cu(II) for each adsorption experiment was made by taking the stock solution using variable volume pipettes, adjusted by diluting with distilled water.

## 2.3 Characterization of the PJS-AC

A spectrophotometer (IR Prestige 21, Shimadzu, Japan) was used for characterization of the PJS-AC. Fourier transform infrared spectroscopy (FTIR) analysis was used to obtain the chemical functional groups from the spectra between 400 and 4000 $cm^{-1}$ of the raw material and the activated carbon. KBr pellets of 0.1% sample were used to determine the sample transmission spectra [26]. Scanning electron microscopy (SEM) (TM-3000, Hitachi, Japan, 500VA, 1 phase 50/60Hz) was used to show the surface micrographs of the raw material.

## 2.4 Cu(II) Adsorption Experiments

Cu(II) adsorption experiments were conducted in batch mode. The same experimental procedure as used in the previous study [26] was used for the Cu(II) adsorption experiments. 1 g of PJS-AC was contacted with 100 ml of Cu(II) solution in a 100-mL Erlenmeyer flask at a stirring speed of 75 rpm. 2-mL samples of Cu(II) solution were taken in a time series (0, 15, 30, 45, 60 and 75 min) using variable volume pipettes and added with 10 mL of distilled water in a 15-mL vial. The Cu(II) concentration of the filtrate was determined by AAS and the concentration of the 2-mL samples of the Cu(II) solution was obtained by multiplying the AAS-based concentration with a dilution factor of 6.

The effect of contact time, ultrasonic assistance, adsorption pH and temperature on the Cu(II) ion adsorption capacity of the adsorbents was investigated. The range of contact time, initial Cu(II) concentration in aqueous solution, pH and temperature of adsorption were 0-80 min, 59.526–1190.532 mg/L (the real concentration of Cu(II) ions based on the AAS analysis and dilution factor), 3-5.5 (± 0.1), and 30-50 °C (± 1 °C), respectively. The Cu(II) aqueous solution pH was adjusted by dropping HCl at a concentration in the range of 0.01-0.5 M (99.8% pure from Gatt-Koller), the solution pH was measured using analytical system Cobra3 Chem-Unit (12153.00, Phywe Systeme, West Germany). To set the adsorption temperature, a SBS multipoint magnetic stirrer was used. A wide range of initial Cu(II) ion concentrations under acidic conditions were applied to obtain the maximum Cu(II) adsorption capacity of the adsorbents [13,19,20,22,29].

Analysis of the data from each experiment was carried out in duplicate, and the average value was taken into account with standard deviation (STDEV in

Excel) in the range of 0.4-0.6. The Cu(II) adsorption isotherm, kinetic and thermodynamic parameters were determined using the experimental data and the related equation.

## 3 Results and Discussion

### 3.1 Functional Groups of the Samples

The FTIR transmission spectra of the raw PJS, PJS-C, PJS-ACWU and PJS-AC are shown in Figure 1. As can be seen in Figure 1, the raw PJS had 8 functional groups. Two bands at a wavenumber of approximately 3635-3765 $cm^{-1}$ with peaks at 3732 and 3645 $cm^{-1}$ were assigned to O-H stretching of hydroxyl groups [17,26,34,35]. These bands had the highest transmittance compared to the other groups, i.e. approximately 96.09 and 95.72%, respectively, showing that phenols were the most dominant functional group in the raw PJS. However, the O-H stretching disappeared in the PJS-C, PJS-ACWU and PJS-AC, inferring that pyrolysis and chemical activation without and with ultrasound assistance completely removed phenols.

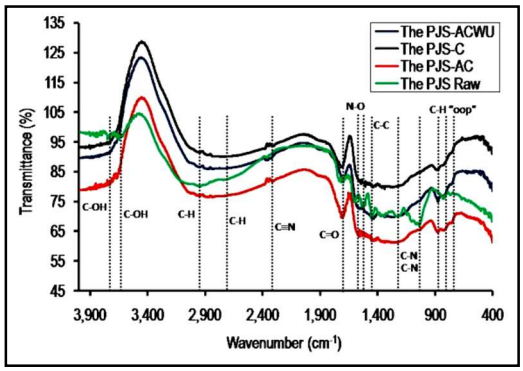


**Figure 1** The FTIR spectra of the PJS raw, PJS-C, PJS-ACWU and PJS-AC.

C–H stretching of alkenes with a weak band at 2865-3005 $cm^{-1}$ and a peak at 2953 $cm^{-1}$ [26,27] existed in the three samples. It is interesting to note that chemical activation without ultrasound increased the transmittance from 80.24 to 87.07%. In contrast, ultrasound assistance decreased it to 77.52%, indicating alkenes being released from the PJS-AC. The C–H stretch of aldehydes at 2830-2695 $cm^{-1}$ with an intense band at 2726 $cm^{-1}$ in the raw PJS was removed in the PJS-C, PJS-ACWU and PJS-AC, while the PJS-AC had the lowest transmittance. The same trend also occurred for the C≡N stretch of nitriles at 2240-2260 $cm^{-1}$ with a peak at 2255 $cm^{-1}$ in the raw PJS, whereas it was completely removed in the PJS-AC. Meanwhile, the C≡N stretch still existed in the PJS-C and PJS-ACWU. It is important to note that ultrasound assistance

resulted in a wider band of C=O stretching at 1665-1760 $cm^{-1}$ with a peak at 1712 $cm^{-1}$. This band is associated to carbonyls [26,36], which were the most dominant functional group in the PJS-AC, even if the transmittance decreased from 86.62% in the PJS-C and 82.07% in the PJS-ACWU to 70.56% in the PJS-AC. This indicates that ultrasound causes carbonyls to also be removed partially from the PJS-AC, and that the presence of carbonyls should let chemical adsorption take place. The same trend of C–H stretching of aldehydes also occurred for the C-H 'oop' stretching of aromatics with triple bands at 675-900 $cm^{-1}$ and peaks at 875, 821 and 709 $cm^{-1}$. These functional groups would also have promoted chemical adsorption on the PJS-AC. The ultrasound assistance also removed the N–O asymmetric stretch (at 1475-1550 $cm^{-1}$ with the peak at 1521 $cm^{-1}$) of nitro compounds, the C–C stretch (at 1400-1500 $cm^{-1}$ with the peak at 1446 $cm^{-1}$) of aromatics, and the C–N stretch (1020-1250 $cm^{-1}$ with 2 peaks at 1226 and 1031 $cm^{-1}$) of aliphatic amines.

Overall, pyrolysis at 500 °C removed almost all functional groups in the raw PJS. The light and volatile matter that may still have been present in the PJS-C was removed further as a result of the chemical activation, as indicated by all transmittance peaks having decreased. Compared to chemical activation without ultrasound assistance, ultrasound assistance should contribute to the formation of more cavities and pores on the PJS-AC. As a result, the Cu(II) ion adsorption capacity of the PJS-AC may be higher than that of the raw PJS and PJS-C. Moreover, chemical adsorption is expected to take place in the presence of some functional groups.

## 3.2 Surface Morphology of Samples

Figures 2(a), (b) and (c) show the SEM analysis for the surface morphology of the PJS-C, PJS-ACWU and PJS-AC, respectively. The PJS-C surface has impurities and the pores are irregular and uneven. The round substances presenting chemical functional groups addressed in previous studies [17,26,37] are not clearly visible on the PJS-C surface. Compared to the PJS-C surface, the PJS-ACWU surface is more clear and clean from impurities as a result of the chemical activation. The wall of the PJS-ACWU surface likely has the same thickness as the wall of the PJS-C surface. There should be more pores on the PJS-ACWU surface as a result of the NaOH dehydrating agent [26], as addressed in the FTIR discussion. Even if Figure 1(b) does not show many pores formed on the wall, Cu(II) ion adsorption capacity of the PJS-ACWU should be higher than that of the PJS-C.

The best surface morphology was shown by the PJS-AC, as can be seen in Figure 2(c). It can be clearly seen that the ultrasound assistance created more irregular and uneven pores, and transport pores were also formed for the PJS-

AC. As expected, in the FTIR result more volatile matter was released because ultrasonics lead NaOH to penetrate deeply into the PJS-AC wall by breaking the stretching of the chemical functional groups on the PJS-CA surface. As a result, the wall of the PJS-AC surface was thinner than that of both the PJS-C and PJS ACWU, and open and transport pores were formed, as can be seen in Figure 2(c). Therefore, Cu(II) ion adsorption capacity of the PJS-AC should be higher than that of both the PJS-C and the PJS ACWU.

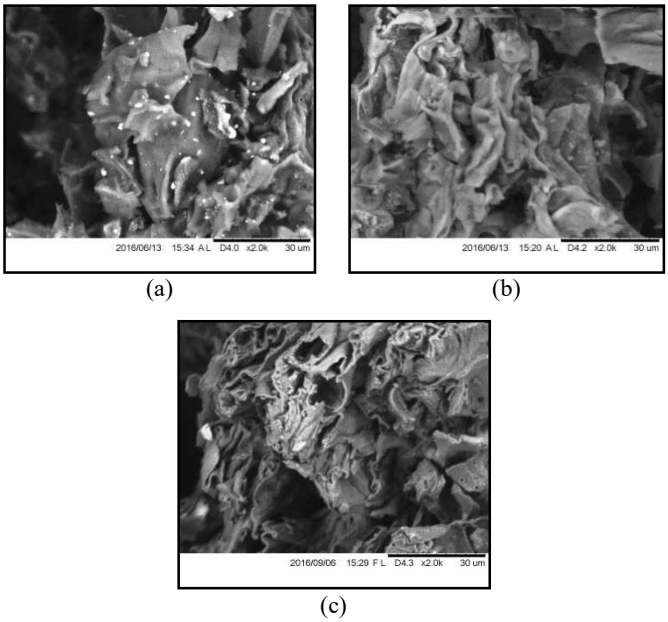


**Figure 2** SEM micrographs of (a) the raw PJS, (b) the PJS-ACWU (c) the PJS-AC.

## 3.3 Effect of Contact Time on Adsorption Capacity

The effect of contact time on the Cu(II) ion adsorption capacity of the PJS-AC is shown in Figure 3. It increased rapidly within 15 min from 0 to 90.78, 92.02 and 93.56 mg/g under the adsorption condition at 30 °C, pH 4.5; 50 °C, pH 4.5; and 30 °C, pH 3, respectively. Following 15 min of contact time, it did not change too much and it reached adsorption equilibrium within 75 min. It is clear that the Cu(II) ion adsorption capacity of the PJS-AC was exponential over contact time, the same as the trend in the previous studies [14,17,38], whereas the adsorbate entered into the PJS-AC pores and was adsorbed rapidly by the active sites in the first 15 min. Due to limited active sites on the surface, Cu(II)

ions were no longer adsorbed during the rest of the contact time, leading to a relatively long time taken for the PJS-AC to adsorb Cu(II) ions.

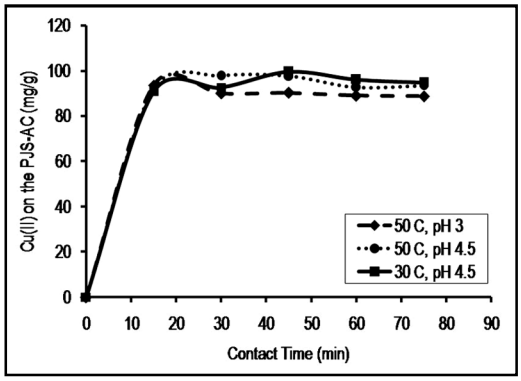


**Figure 3** Cu(II) ion adsorption capacity of the PJS-AC over contact time. Operation conditions: 100 mL Cu(II) aqueous solution at 1190.532 mg/L, 1 g the PJS-AC, contact time of 0-75 min, adsorption temperature at 30 and 50 °C (± 1 °C), 75-rpm stirring speed, pH 3 and 4.5, and 1 atm. STDEV = 0.4.

## 3.4 Effect of Ultrasound on Adsorption Capacity

Figure 4 shows the effect of ultrasound on Cu(II) ion adsorption capacity. The Cu(II) adsorption capacity increased by 5.18% from 82.76 to 87.05 mg/g for chemical activation without ultrasound assistance. It increased by 14.07% as a result of ultrasound assistance. As expected, in the FTIR and SEM analyses the Cu(II) ion adsorption capacity by the PJS-AC was higher than that of both the PJS-C and PJS ACWU, i.e. 94.40 mg/g.

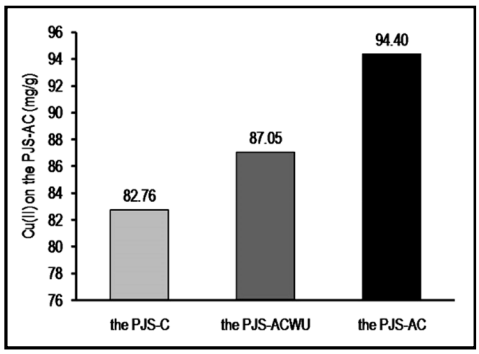


**Figure 4** Cu(II) ion adsorption capacity of the PJS-C, PJS-ACWU and PJS-AC at equilibrium time. Operation conditions: 100 mL Cu(II) aqueous solution at 1190.532 mg/L, 1 g adsorbent, 75-min contact time, adsorption temperature at 30 °C (± 1 °C), 75-rpm stirring speed, pH 5.5, and 1 atm. STDEV = 0.5.

## 3.5 Effect of Initial Solution pH on Adsorption Capacity

Previous studies have shown that Cu(II) ion adsorption onto adsorbents reaches maximum adsorption capacity in acid conditions of the initial solution [13,21,22,24]. Hence, the effect of initial solution pH on the Cu(II) adsorption capacity of the PJS-AC was investigated in a pH range of 3-5.5. The result as depicted in Figure 5 shows that the pH of the initial solution dynamically affected the Cu(II) adsorption capacity and that the pH effect was almost the same for different adsorption temperatures. It increased moderately from approximately 91.65 to 94.81 mg/g at a pH of 3-4.5 for adsorption temperature at 30 °C, and from 88.76 to 93.46 mg/g for adsorption temperature at 50 °C. Lifting the pH to 5.5 decreased it to 94.40 and 91.67 mg/g for adsorption temperature at 30 and 50 °C, respectively. The maximum Cu(II) adsorption capacity was found at a pH of 4.5, i.e. 0.5 higher than the pH for the maximum Cu(II) adsorption capacity of activated water melon [13] and biomass residue-based activated carbon [22].

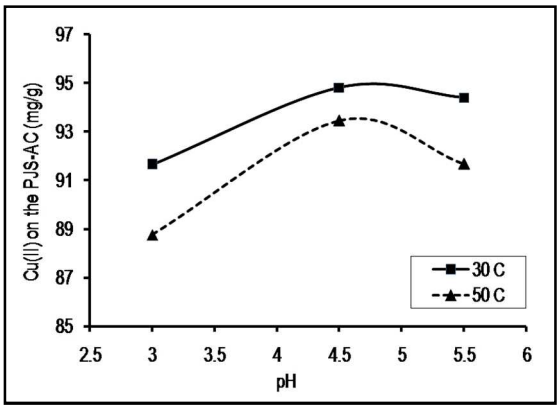


**Figure 5** Cu(II) ion adsorption capacity over pH of initial solution. Operation conditions: 100 mL Cu(II) aqueous solution at 1190.532 mg/L, 1 g adsorbent, 75-min contact time, adsorption temperature at 30 and 50 °C (± 1 °C), 75-rpm stirring speed, pH of 3-5.5, and 1 atm. STDEV = 0.5.

## 3.6 Effect of Temperature on Adsorption Capacity

Figure 5 also shows that the adsorption temperature influenced the Cu(II) adsorption capacity. All values of Cu(II) adsorption capacity at 50 °C of adsorption temperature were lower than the values of Cu(II) adsorption capacity at 30 °C. In other words, rising the adsorption temperature decreased the adsorption of Cu(II) ions onto the PJS-AC. For example, it was approximately 94.40 and 91.67 mg/g at 30 and 50 °C, respectively for a pH of 5.5. It was 94.81 and 93.46 mg/g, respectively for a pH of 4.5, and it was 91.65 and 88.76 mg/g

for a pH of 3.0, respectively. However, the result shown was only for the initial Cu(II) concentration at 2381.065 mg/L. The temperature effect is discussed further in the next sections.

### 3.7 Cu(II) Adsorption Isotherm of the PJS-AC

The common models of the Langmuir and Freundlich adsorption isotherms were used for determining the related parameters. The Langmuir equation [26,39] can be expressed in linear form [37] as:

$$\frac{C_e}{q_e} = \frac{1}{q_m K_L} + \frac{1}{q_m} C_e \tag{1}$$

where $C_e$ (mg/L) is the equilibrium Cu(II) concentration in solution, $q_e$ (mg/g) presents the adsorption capacity, $q_m$ (mg/g), as the Langmuir monolayer adsorption capacity, and $K_L$ (L/mg) denotes the Langmuir constant. The parameter values were worked out using the intercept, $1/(q_m K_L)$, and the slope, $1/q_m$, of the straight line $C_e/q_e$ versus $C_e$, as revealed in Figure 6(a). Both the nature of Cu(II) ion adsorption onto the PJS-AC and the adsorption isotherm type were obtained using the expression $R_L = 1/(K_L C_o + 1)$, where $C_o$ (mg/L) is the highest initial concentration of Cu(II) in aqueous solution. When the $R_L = 0$, $0 < R_L < 1$, $R_L = 1$, or $R_L > 0$ [40] the Cu(II) adsorption on the PJS-AC should be irreversible, favorable, linear, or unfavorable, respectively. The Freundlich equation [26,41,42] can be expressed in linearized form as:

$$\log q_e = \frac{1}{n} \log C_e + \log K_F \tag{2}$$

where $K_F$ (L/mg) represents the Freundlich constant and $1/n$ denotes the adsorption intensity. The values of the Freundlich parameters were determined using the intercept, $\log K_F$, and the slope, $1/n$, of the straight line of $\log q_e$ versus $\log C_e$, as can be seen in Figure 6(b).

All values of both adsorption isotherm parameters are listed in Table 1. As shown by the legend in Figure 6 and listed in Table 1, the average correlation coefficient $R^2$ for the Langmuir adsorption isotherm was 0.889, a bit lower than the average Freundlich $R^2$, which was 0.941. This indicates that the Freundlich expression model provided the best fit for the adsorption of Cu(II) ions onto the PJS-AC. However, Langmuir adsorption may take place, since when the $R^2$ was still high, the adsorption capacity, $q_m$, was close to the one presented in Figure 3. In addition, temperature and pH effects on adsorption capacity were the same as the ones presented in Figure 4. Increasing the adsorption temperature lowered the adsorption capacity and the maximum adsorption capacity was reached at a pH of 4.5.

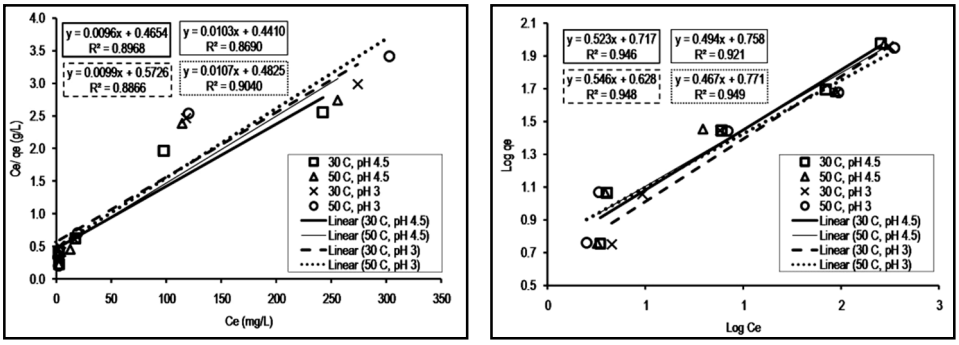


(a) (b)

**Figure 6** Adsorption isotherm expression of (a) Langmuir and (b) Freundlich for Cu(II) ion adsorption onto the PJS-AC. Operation conditions: 100 mL Cu(II) aqueous solution at 1190.532 mg/L, 1 g adsorbent, 75-min contact time, adsorption temperature at 30 and 50 °C (± 1 °C), 75-rpm stirring speed, pH of 3-5.5, and 1 atm. STDEV = 0.4.

**Table 1** Cu(II) adsorption isotherm parameters based on Langmuir and Freundlich models.

| T ($^oC$) | pH | Langmuir | | | Freunclich | | |
|---|---|---|---|---|---|---|---|
| | | $q_m$ (mg/g) | $K_L$ (L/mg) | $R^2$ | $1/n$ | $K_F$ (L/mg) | $R^2$ |
| 30 | 3 | 101.010 | 0.017 | 0.887 | 0.546 | 4.246 | 0.948 |
| 50 | 3 | 93.458 | 0.022 | 0.904 | 0.467 | 5.902 | 0.949 |
| 30 | 4.5 | 104.167 | 0.021 | 0.897 | 0.523 | 5.212 | 0.946 |
| 50 | 4.5 | 97.087 | 0.023 | 0.869 | 0.494 | 5.727 | 0.921 |

Meanwhile, using the average Langmuir constant ($K_L$) obtained (0.039), confirmed that the Langmuir isotherm is also favorable for adsorption of Cu(II) by the PJS-AC. The highest Cu(II) adsorption capacity of the PJS-AC was 104.167 mg/g at 30 °C and pH 4.5 with the Langmuir constant at 0.523 L/mg, Freundlich adsorption intensity at 0.523, and the Freundlich constant at 5.212 L/mg.

## 3.8 Cu(II) Adsorption Kinetic of the PJS-AC

The linearized pseudo first-order kinetic equation (PFOKE) by Lagergren [43], given as Eq. (3) [17,26], and the linearized pseudo second-order kinetic equation (PSOKE) [44], given as Eq. (4) [17,26,45], were used to obtain the parameters.

$$\log(q_e - q_t) = \log q_e - \left(\frac{k_L t}{2.303}\right) \tag{3}$$

$$\frac{t}{q_t} = \frac{1}{k_H q_e^{\,2}} + \frac{t}{q_e} \tag{4}$$

where $q_t$ (mg/g) represents Cu(II) ion adsorption capacity of the PJS-AC at time $t$ (min), $q_e$ (mg/g) is the Cu(II) ion adsorption capacity at equilibrium, $k_L$ (/min) is the PFOKE adsorption rate constant, and $k_H$ (g/mg.min) denotes the PSOKE adsorption rate constant. The values of $q_e$, $k_L$, or $k_H$ were determined using the slope and intercept of related Eqs. (3) or (4), and all the parameter values are listed in Table 2.

**Table 2** Cu(II) Ion Adsorption Kinetic Parameters based on PFOKE and PSOKE

| T (°C) | pH | PFOKE | | | PSOKE | | |
|---|---|---|---|---|---|---|---|
| | | $q_e$ (mg/g) | $k_L$ (/min) | $R^2$ | $q_e$ (mg/g) | $k_H$ (g/mg.min) | $R^2$ |
| 30 | 3 | 9.682 | 0.042 | 0.391 | 91.743 | 0.487 | 0.999 |
| 50 | 3 | 10.483 | 0.043 | 0.428 | 88.496 | 0.157 | 0.999 |
| 30 | 4.5 | 22.465 | 0.053 | 0.702 | 96.154 | 0.200 | 0.998 |
| 50 | 4.5 | 12.517 | 0.049 | 0.499 | 93.458 | 0.156 | 0.998 |

Operation conditions: 100 mL Cu(II) aqueous solution with a predetermined concentration of 1190.532 mg/L, 1 g of PJS-AC, contact time of 0-75 min, adsorption temperature at 30 and 50 °C (± 2 °C), 75 rpm magnetic stirring, pH 3 and 4.5 (± 0.1), and 1 atm.

As shown in Table 2, the PSOKE gave the best fit for Cu(II) ion adsorption onto the PJS-AC, indicated by the average $R^2$ value of 0.998. The same effect of adsorption temperature and pH on adsorption capacity in the adsorption isotherm was also found in the adsorption kinetic.

Increasing the adsorption temperature decreased the Cu(II) ion adsorption capacity of the PJS-AC, while the maximum adsorption capacity (96.154 mg/g) was reached at 30 °C and pH 4.5 with the PSOKE adsorption rate constant at 0.200 g/mg.min.

## 3.9 Cu(II) Adsorption Thermodynamics

Thermodynamic equations of Eqs. (5), (6) and (7) were used to work out the change of enthalpy ($\Delta H^0$), free energy ($\Delta G^0$) and entropy ($\Delta S^0$) for Cu(II) adsorption onto the PJS-AC. The $\Delta H^0$ (J/mol) value was obtained using Eq. (5) of the Van 't Hoff linear model [38]:

$$\ln K_d = \frac{\Delta S^0}{R} - \frac{\Delta H^0}{RT} \tag{5}$$

where $K_d$ (L/mg) is defined as distribution coefficient ($q_e/C_e$) at a temperature of $T$ (K) with $q_e$ and $C_e$ given at the maximum initial concentration of the

Langmuir plot for the Cu(II) ion adsorption isotherm, and $R$ denotes the ideal gas constant (8.314 J/mol K). The values of $C_{e1}$, $C_{e3}$, $q_{e1}$, $q_{e3}$, $K_{d1}$, $K_{d3}$, $T_1$, and $T_3$, were approximately 242.394 mg/L, 255.954 mg/L, 94.814 mg/g, 93.478 mg/g, 0.391 L/g, 0.365 L/g, 303.15 K and 333.15 K, respectively, taken from the Langmuir adsorption isotherm at pH 4.5, as presented in Figure 6(a). The notations $C_{e1}$ and $C_{e3}$ represent the equilibrium Cu(II) concentration in the solution at an adsorption temperature of $T_1$ and $T_3$, respectively, as well as the notations for $q_{e1}$ and $q_{e3}$, $K_{d1}$ and $K_{d3}$. An additional adsorption isotherm experiment was conducted at 315.15 K (denoted as $T_2$). The values of $C_{e2}$, $q_{e2}$, $K_{d2}$ and $T_2$ obtained were 248.871 mg/L, 94.166 mg/g and 0.378 L/g, respectively.

As a result, the trendline equation obtained was $\ln k_d = 230.22/\mathrm{T} - 1.70$ and the value of $\Delta H^0$ was –1.914 kJ/mol. The positive value of $\Delta H^0$ indicates the exothermic nature of the adsorption of Cu(II) by the PJS-AC. This is reasonable because the entrophy decreases when the Cu(II) ions are adsorbed, leading to the negative value of enthalpy [46,47]. The increase in temperature from 303.15 to 333.15 K causes a decrease in the Langmuir-based Cu(II) adsorption capacity from 104.167 to 97.087 mg/g (highlighted in Section 3.6), which is also reasonable according to Le Chatelier's principle for chemical adsorption [48], and the activation energy should have a positive sign [49]. The activation energy (E) was obtained using the linear plot slope of the trendline of $1/T$ versus $\ln q_m$ as given in Eq. (6):

$$\ln q_m = q_{mi} - \frac{E}{R}\left(\frac{1}{T}\right) \tag{6}$$

where $q_{\mathrm{mi}}$ (mg/g) is the Langmuir-based Cu(II) adsorption capacity at temperature $T$ [48,50]. The values of $q_{\mathrm{m1}}$, $q_{\mathrm{m2}}$, $q_{\mathrm{m3}}$, $T_1$, $T_2$ and $T_3$ were 104.167, 100.561, 97.087 mg/g, 303.15, 315.15 and 333.15 K, respectively. The trendline equation obtained was $\ln q_m = 235.08/\mathrm{T} + 3.87$, and the $E$ value obtained from the slope was –1.954 kJ/mol. The negative sign of $E$ indicates exothermic chemical adsorption taking place in the Cu(II) adsorption onto the PJS-AC, and could refer to monolayer Langmuir adsorption [51].

The $\Delta S^0$ value determined using Eq. (5) was –0.141 kJ/mol.K. A negative sign of $\Delta S^0$ corresponds to a decrease in the degree of freedom [46,47]. Meanwhile, the $\Delta G^0$ (J/mol) can be obtained using Eq. (7) [52]:

$$\Delta S^0 = \frac{\Delta H^0 - \Delta G^0}{T} \tag{7}$$

The $\Delta G^0$ values obtained using Eq. (7), $\Delta S^0$ at -0.141 kJ/mol.K and $\Delta H^0$ at – 1.914 kJ/mol were 40.932 and 45.172 kJ/mol for an adsorption temperature of 300.15 and 318.15 K, respectively. The positive sign of the $\Delta G^0$ values confirms that the Cu(II) adsorption onto the PJS-AC was a non-spontaneous process.

## 3.10 Cu(II) Adsorption Capacity by Various Activated Carbons

A comparison of Cu(II) adsorption capacity by various activated carbons prepared from lignocellulosic material is listed in Table 3.

**Table 3** Adsorption of Cu(II) by activated carbons.

| Activated Carbon | T (°C) | pH | $q_m$ (mg/g) | Ref. |
|---|---|---|---|---|
| PJS-AC, USAC-NaOH | 30 | 4.5 | 104.167 | PS |
| WM-AC, $Ca(OH)_2$, USAD | 30 | 5 | 31.025 | [13] |
| WM-AC, $C_6H_8O_7$, USAD | 30 | 5 | 27.027 | [13] |
| CRFB-AC, $ZnCl_2$ | RT | 5 | 23.100 | [21] |
| PC-AC, $ZnCl_2$ | RT | 5 | 5.100 | [21] |
| TDS-AC, $H_3PO_4$ | 40 | 5 | 31.250 | [22] |
| HH-AC, $ZnCl_2$ | 18 | 5.7 | 6.650 | [23] |
| HS-AC, $H_2SO_4$ | 50 | 6 | 58.270 | [24] |
| APC-AC, NaOH | 25 | 5 | 26.710 | [26] |
| ACS-AC, NaOH | 27 | 6.5 | 50.51 | [50] |
| ACS-AC, NaOH | 45 | 6.5 | 55.25 | [50] |
| GCF-AC, $H_2SO_4$ | NA | 4 | 15.470 | [53] |
| AS-AC, $H_2SO_4$ | NA | 6.5 | 22.800 | [53] |
| RWS-AC, $H_3PO_4$ | NA | 6 | 5.720 | [54] |

The abbreviations PS, AC, NA, RT, USAC and USAD stand for *present study*, *activated carbon*, *not available*, *room temperature*, *ultrasound-assisted activation*, and *ultrasound assisted adsorption*, respectively. The abbreviations WM, CRFB, CP, TDS, HH, HS, APC, GCF, AS, RWS and ACS stand for *watermelon*, *carbon residue from biomass gasification*, *commercial powder*, *Tunisian date stones*, *hazelnut husks*, *hazelnut shell*, *Australian pine cone*, *granular commercial Filtrasorb 200*, *apricot stone*, *rubber wood sawdust* and *areca catechu shell*, respectively. As shown in Table 3, the Cu(II) adsorption capacity of the PJS-AC was the highest compared to those of the other activated carbons prepared from lignocellulosic materials listed in Table 1. This finding as well as the application of ultrasound in activation could be a significant contribution to the development of activated carbon based on lignocellulosic materials. Further studies of elemental analysis, surface area, pore volume and average pore diameter of PJS-AC are worthy for future research.

## 4 Conclusion

This study presented adsorption of Cu(II) ions onto activated carbon derived from Pithecellobium jiringa shell (PJS-AC). Using ultrasound for the activation released almost all the light and volatile matter in the PJS-AC, as was shown by FTIR analysis, and it produced more cavities and pores on the PJS-AC, confirmed by SEM analysis. The Freundlich isotherm (average $R^2$ = 0.941) fitted better compared to the Langmuir isotherm (average $R^2$ = 0.889) showing that physical sorption was dominant compared to chemical sorption. The Cu(II) adsorption kinetic fitted well to the PSOKE (average $R^2$ = 0.998). The highest Cu(II) ion adsorption capacity of the PJS-AC was 104.167 mg/g with the Langmuir constant at 0.523 L/mg at 30 °C and pH 4.5. The Freundlich adsorption intensity and constant were 0.523 and 5.212 L/mg, respectively. The maximum adsorption capacity based on the PSOKE was 96.154 mg/g with the rate constant at 0.200 g/mg.min at 30 °C and pH at 4.5. The thermodynamic parameters showed that Cu(II) adsorption onto the PJS-AC was exothermic chemical adsorption in part. The degree of freedom decreased and the adsorption was non-spontaneous.

## Acknowledgements

The authors would like to fully thank the Chemical Engineering Department and the Mining Engineering Department of Syiah Kuala University for the technical support in the experimental work and the Mechanical Engineering Department of Syiah Kuala University for the SEM analysis. Finally, we also wish to thank the Mathematics and Science Faculty of Syiah Kuala University for the AAS analysis.

## References

[1] Hawkes, S.J., *What is a Heavy Metal?,* Journal of Chemical Education, **74**(11), pp. 1374-1380, 1997.

[2] Srivastava, N.K. & Majumder, C.B., *Novel Biofiltration Methods for the Treatment of Heavy Metals from Industrial Wastewater*, Journal of Hazardous Materials, **151**(1), pp. 1-8, 2008.

[3] Munaf, E. & Takeuchi, T., *Monitoring of University Effluents*, In: Hazardous Waste Control in Research and Education, Korenaga, T., Tsukube, H., Shinoda, S. & Nakamura, I., eds. Boca Raton, FL: CRC Press, 1994.

[4] Bala, M., Shehu, R.A. & Lawal, M., *Determination of the Level of Some Heavy Metals in Water Collected from Two Pollution - Prone Irrigation Areas Around Kano Metropolis*, Bayero Journal of Pure and Applied Sciences, **1**(1), pp. 6-38, 2008.

[5] Gua, Y.B, Feng, H., Chen, C., Jia, C.J., Xiong, F. & Lu, Y., *Heavy Metal Concentration in Soil and Agricultural Products Near an Industrial District*, Polish Journal of Environmental Studies, **22**(5), pp. 1357-1362, 2013.

[6] Lakherwal, D., *Adsorption of Heavy Metals: A Review*, International Journal of Environmental Research and Development, **4**(1), pp. 41-48, 2014.

[7] Theophanides, T. & Anastassopoulou, J., *Copper and Carcinogenesis*, Critical Reviews in Oncology/Hematology, **42**(1), pp. 57-64, 2002.

[8] Carl, L.K., Harry, J.M. & Elizabeth, M.W., *A Review: The Impact of Copper on Human Health*, New York: International Copper Association Ltd., 2003.

[9] Minamisawa, M., Minamisawa, H., Yoshida, S. & Takai, N., *Adsorption Behavior of Heavy Metals on Biomaterials*, Journal of Agricultural and Food Chemistry, **52**(18), pp. 5606-5611, 2004.

[10] Tobin, J.M. & Roux, J.C., *Mucor Biosorbent for Chromium Removal*, Water Research, **32**(5), pp. 1407–1416, 1998.

[11] Leung, W.C., Wong, M.F., Chua, H., Lo, W., Yu, P.H.F. & Leung, C.K., *Removal and Recovery of Heavy Metals by Bacteria Isolated from Activated Sludge Treating Industrial Effluents and Municipal Wastewater*, Water Science and Technology, **41**(12), pp. 233-240, 2000.

[12] Eccles, H., *Treatment of Metal-Contaminated Wastes: Why Select a Biological Process?,* Trends in Biotechnology, **17**(12), pp. 462-465, 1999.

[13] Gupta, H. & Gogate, P.R., *Intensified Removal of Copper from Waste Water Using Activated Water Melon Based Biosorbent in The Presence of Ultrasound*, Ultrasonics Sonochemistry, **30**, pp. 113-122, 2016.

[14] Wong, K.K., Lee, C.K., Low, K.S. & Haron, M.J., *Removal of Cu and Pb by Tartaric Acid Modified Rice Husk from Aqueous Solution*, Chemosphere, **50**(1), pp. 23-28, 2003.

[15] Basso, M.C., Cerrella, E.G. & Cukierman, A.L., *Lignocellulosic Materials as Potential Biosorbents of Trace Toxic Metals from Wastewater*, Industrial and Engineering Chemistry Research, **41**(15), pp. 3580-3585, 2002.

[16] Baquero, M.C., Giraldo, L., Moreno, J.C., Suárez-García, F., Martínez-Alonso, A. & Tascón, J.M.D., *Activated Carbons by Pyrolysis of Coffee Bean Husks in Presence of Phosphoric Acid*, Journal of Analytical and Applied Pyrolysis, **70**(2), pp. 779-784, 2003.

[17] Muslim, A., Zulfian, Ismayanda, M.H., Devrina, E. & Fahmi, H., *Adsorption of Cu(II) from The Aqueous Solution by Chemical Activated Adsorbent of Areca Catechu Shell*, Journal of Engineering Science and Technology, **10**(12), pp. 1654-1666, 2015.

[18] Research In China., *China Activated Carbon Industry Report*, 2014-2017, 2015.
[19] Moreno-Pirajan, J.C. & Giraldo, L., *Adsorption of Copper from Aqueous Solution by Activated Carbons Obtained by Pyrolysis of Cassava Peel*, Journal of Analytical and Applied Pyrolysis, **87**(2), pp. 188-193, 2010.
[20] Klasson, K.T., Wartelle, L.H., Rodgers, J.E. & Lima, I.M., *Copper(II) Adsorption by Activated Carbons from Pecan Shells: Effect of Oxygen Level During Activation*, Industrial Crops and Products, **30**(1), pp. 72-77, 2009.
[21] Runtti, H., Tuomikoski, S., Kangas, T., Lassi, U., Kuokkanen, T. & Rämö, J., *Chemically Activated Carbon Residue from Biomass Gasification as A Sorbent for Iron(II), Copper(II) and Nickel(II) Ions*, Journal of Water Process Engineering, **4**, pp. 12-24, 2014.
[22] Bouhamed, F., Elouear, Z. & Bouzid, J., *Adsorptive Removal of Copper(II) from Aqueous Solution on Activated Carbon Prepared from Tunisian Date Stones: Equilibrium, Kinetic and Thermodynamics*, Journal of the Taiwan Institute of Chemical Engineers, **43**(5), pp. 741-749, 2012.
[23] Imamoglu, M. & Tekir, O., *Removal of Copper (II) and Lead (II) Ion from Aqueous Solution by Adsorption on Activated Carbon from a New Precursor Hazelnut Husks*, Desalination, **228**(1-3), pp. 108-113, 2008.
[24] Demirbas, E., Dizge, N., Sulak, M.T. & Kobya, M., *Adsorption Kinetic and Equilibrium of Copper from Aqueous Solution Using Hazelnut Shell Activated Carbon*, Chemical Engineering Journal, **148**(2-3), pp. 480-487, 2009.
[25] Milenković, D.D., Bojić, A.L.J. & Veljković, V.B., *Ultrasound-Assisted Adsorption of 4-Dodecylbenzene Sulfonate from Aqueous Solution by Corn Cob Activated Carbon*, Ultrasonics Sonochemistry, **20**(3), pp. 955-962, 2013.
[26] Muslim, A., *Australian Pine Cones-Based Activated Carbon for Adsorption of Copper in Aqueous Solution*, Journal of Engineering Science and Technology, **12**(2), pp. 280-295, 2017.
[27] Lim, T.K., *Archidendron Jiringa*, *Edible Medicinal and Non-Medicinal Plants*, Springer Netherlands, pp. 544-548, 2012.
[28] BPS - Statistics Indonesia, *Vegetables Production in Indonesia*, 2009–2013, 2015. http://i-pc.ilmci.com/file/2015/02/PR_Sayuran_ ATAP.pdf
[29] Kurniawan, T.A., Chan, G.Y.S., Lo, W.H. & Babel, S., *Comparisons of Low-Cost Adsorbents for Treating Waste Waters Laden with Heavy Metals*, Science of the Total Environment, **366**(2-3), pp. 409-426, 2006.
[30] Dehdashti, A., Khavanin, A., Rezaee, A. & Asilian, H., *Regeneration of Granular Activated Carbon Saturated with Gaseous Toluene by Microwave Irradiation*, Journal of Engineering Environmental Science, **34**, pp. 49-58, 2010.

[31] Hesas, R.H., Daud, W.M.A.W., Sahu, J.N. & Arami-Niya, A., *The Effects of a Microwave Heating Method on the Production of Activated Carbon from Agricultural Waste: A Review*, Journal of Analytical and Applied Pyrolysis, **100**, pp. 1-11, 2013.

[32] Chen, C.J., Wei, L.B., Zhao, P.C., Li, Y., Hu, H.Y. & Qin, Y.B., *Study on Preparation of Activated Carbon from Corncob Furfural Residue with $ZnCl_2$ by Microwave Irradiation*, New Materials and Advanced Materials, **152-153**(1-2), pp. 1322-1327, 2011.

[33] Commenges-Bernole, N. & Marguerie, J., *Adsorption of Heavy Metals on Sonicated Activated Sludge*, Ultrasonics Sonochemistry, **16**(1), pp. 83-87, 2009.

[34] Lee, H.W., Insyani, R., Prasetyo, D., Prajitno, H. & Sitompul, J.P., *Molecular Weight and Structural Properties of Biodegradable PLA Synthesized with Different Catalysts by Direct Melt Polycondensation*, Journal of Engineering and Technological Sciences, **47**(4), pp. 364-373, 2015.

[35] Yang, T. & Lua, A.C., *Characteristics of Activated Carbons Prepared from Pistachio-Nut Shells by Physical Activation*, Journal of Colloid and Interface Science, **267**(2), pp. 408-417, 2003.

[36] Chakravarty, P., Sarma, N.S. & Sarma, H.P., *Removal of Lead(II) from Aqueous Solution Using Heartwood of Areca Catechu Powder*, Desalination, **256**(1-3), pp. 16-21, 2010.

[37] Zengin, A., Akalin, M.K., Tekin, K., Erdem, M., Turga, T. & Karagoz, K., *Preparation and Characterization of Activated Carbons from Waste Melamine Coated Chipboard by Koh Activation*, Ekoloji, **21**(85), pp. 123-128, 2012.

[38] Mengistie, A.A., Siva, R.T., Prasada, R.A.V. & Malairajan, S., *Removal of Lead(II) Ion from Aqueous Solution Using Activated Carbon from Militia Ferruginea Plant Leaves*, Bulletin of the Chemical Society of Ethiopia, **22**(3), pp. 349-360, 2008.

[39] Langmuir, I., *The Adsorption of Gases on Plane Surface of Glass, Mica and Platinum*, Journal of the American Chemical Society, **40**(9), pp. 1361-1403, 1918.

[40] Karagoz, S., Tay, T., Ucar, S. & Erdem, M., *Activated Carbons from Waste Biomass by Sulfuric Acid Activation and Their Use on Methylene Blue Adsorption*, Bioresource Technology, **99**(14), pp. 6214-6222, 2008.

[41] Freundlich, H.M.F., *Over the Adsorption in Solution*, The Journal of Physical Chemistry, **57**, pp. 385-471, 1906.

[42] Silverstein, R.M., Bassler, G.C. & Morrill, T.C., *Spectrometric Identification of Organic Compounds*, 4th ed., New York: John Wiley and Sons, 1981.

[43] Lagergren, S., *About the Theory of So-Called Adsorption of Soluble Substances*, Kungliga Svenska Vetenskapsakademies Handlingar, **24**(4), pp. 1-39, 1898.
[44] Ho, Y.S., Wase, D.A.J. & Forster, C.F., *Kinetic Studies of Competitive Heavy Metal Adsorption by Sphagnum Moss Peat*, Environmental Technology, **17**(1), pp. 71-77, 1996.
[45] Rajamohan, N., Rajasimman, M., Rajeshkannan, R. & Sivaprakash, B., *Kinetic Modeling and Isotherm Studies on a Batch Removal of Acid Red 114 by an Activated Plant Biomass*, Journal of Engineering Science and Technology, **8**(6), pp. 778-792, 2013.
[46] Papirer, E., *Adsorption on Silica Surfaces: Surfactant Science Series*, New York, USA: Marcel Dekker, Inc., 2000.
[47] Kumar, A. & Awasthi, A., *Bioseparation Engineering*, New Dehli, India: I.K. International Publishing House, Pvt. Ltd., 2009.
[48] Rao, S.R., *Surface Chemistry of Froth Flotation*, **1**, Fundamentals, New York, USA: Springer Science, 2004.
[49] Tan, I.A.W., Ahmad, A.L. & Hameed, B.H., *Adsorption Isotherm, Kinetic, Thermodynamics and Desorption Studies of 2,4,6-Trichlorophenol on Oil Palm Empty Fruit Bunch-Based Activated Carbon*, Journal of Hazardous Materials, **164**(2-3), pp. 473-482. 2009.
[50] Muslim, A., Aprilia, S., Suha, T.A. & Fitri Z., *Adsorption of Pb(II) Ions from Aqueous Solution Using Activated Carbon Prepared from Areca Catechu Shell: Kinetic, Isotherm and Thermodynamic Studies*, Journal of the Korean Chemical Society, **61**(3), pp. 89-96, 2017.
[51] Worch, E., *Adsorption Technology in Water Treatment: Fundamentals, Processes, and Modeling*, Berlin: Walter de Gruyter, 2012.
[52] Mohan, D., Gupta, V.K., Srivastava, S.K. & Chander, S., *Kinetic of Mercury Adsorption from Waste Water Using Activated Carbon Derived from Fertilizer Waste*, Colloids and Surfaces, **177**(2-3), pp. 169-181, 2001.
[53] Bansode, R.R., Losso, J.N., Marshall, W.E., Rao, R.M. & Portier, R.J., *Adsorption of Metal Ions by Pecan Shell-Based Granular Activated Carbons*, Bioresource Technology, **89**(2), pp. 115-119, 2003.
[54] Kobya, M., Demirbas, E., Senturk, E. & Ince, M., *Adsorption of Heavy Metal Ions from Aqueous Solutions by Activated Carbon Prepared from Apricot Stone*, Bioresource Technology, **96**(13), pp. 1518-1521, 2005.